Title
Visceral Mechano-sensing Neurons Control Drosophila Feeding by Using Piezo as a Sensor

Journal
Neuron, 108(4)

ISSN
0896-6273

Authors
Wang, Pingping
Jia, Yinjun
Liu, Ting
et al.

Publication Date
2020-11-01

DOI
10.1016/j.neuron.2020.08.017

Peer reviewed

HHS Public Access

Author manuscript

Neuron. Author manuscript; available in PMC 2021 November 25.

Published in final edited form as:

Neuron. 2020 November 25; 108(4): 640–650.e4. doi:10.1016/j.neuron.2020.08.017.

Visceral Mechano-sensing Neurons Control *Drosophila* Feeding by Using Piezo as a Sensor

Pingping Wang[1], **Yinjun Jia**[1], **Ting Liu**[1], **Yuh-Nung Jan**[2,*], **Wei Zhang**[1,3,*]

[1]School of Life Sciences, Tsinghua-Peking Joint Center for Life Sciences, IDG/McGovern Institute for Brain Research, Tsinghua University, Beijing, 100084, China

[2]Howard Hughes Medical Institute, Departments of Physiology, Biochemistry and Biophysics, University of California, San Francisco, San Francisco, CA 94158, USA

[3]Lead Contact

SUMMARY

Animal feeding is controlled by external sensory cues and internal metabolic states. Does it also depend on enteric neurons that sense mechanical cues to signal fullness of the digestive tract? Here, we identify a group of *piezo*-expressing neurons innervating the *Drosophila* crop (the fly equivalent of the stomach) that monitor crop volume to avoid food overconsumption. These neurons reside in the pars intercerebralis (PI), a neuro-secretory center in the brain involved in homeostatic control, and express insulin-like peptides with well-established roles in regulating food intake and metabolism. Piezo knockdown in these neurons of wild-type flies phenocopies the food overconsumption phenotype of *piezo*-null mutant flies. Conversely, expression of either fly Piezo or mammalian Piezo1 in these neurons of *piezo*-null mutants suppresses the overconsumption phenotype. Importantly, Piezo+ neurons at the PI are activated directly by crop distension, thus conveying a rapid satiety signal along the “brain-gut axis” to control feeding.

Graphical Abstract

*Correspondence: yuhnung.jan@ucsf.edu (Y.-N.J.), wei_zhang@mail.tsinghua.edu.cn (W.Z.).

AUTHOR CONTRIBUTIONS

P.W., T.L., and W.Z. performed the experiments and analyzed data. Y.J. helped with FlyPAD data analysis and single-cell labeling. Y.N.-J. and W.Z. wrote the manuscript. All authors discussed and commented on the manuscript.

SUPPLEMENTAL INFORMATION

Supplemental Information can be found online at https://doi.org/10.1016/j.neuron.2020.08.017.

DECLARATION OF INTERESTS

The authors declare no competing interests.

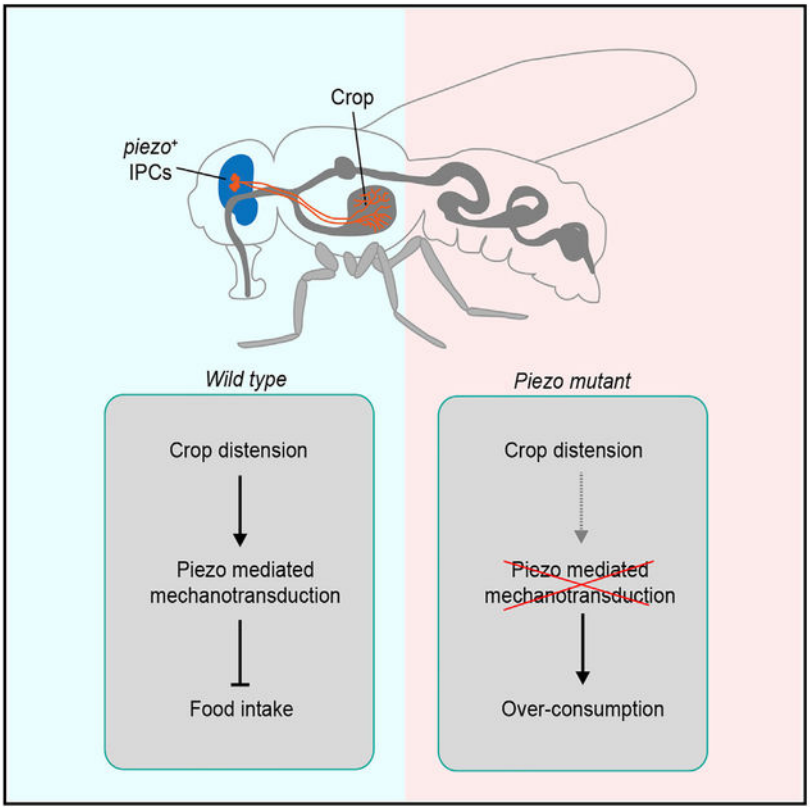

In Brief

Wang et al. identify a group of Piezo-expressing neurons in the fly brain that directly innervate the crop. These mechanosensitive neurons monitor crop volume change during feeding to avoid overconsumption.

INTRODUCTION

Food intake is regulated by feedback from both gustatory organs and the gastrointestinal (GI) tract (Travers et al., 1987; Kim et al., 2018). Neuronal and humoral signals that encode food palatability control feeding in a temporally and spatially specific manner (Asher and Sassone-Corsi, 2015), and the satiety signal following food ingestion is thought to be mediated by mechanical stimulation of the GI tract and by peptide release through the chemical effects of food (Williams et al., 2016; Xu and Xie, 2016). Although there is increasing understanding of how chemical cues released by the GI tract or the brain confer a sense of satiety and inhibit feeding, far less is known about the role of mechano-sensing in the regulation of food intake.

In mammals, parasympathetic innervations of the GI tract via the vagus nerve coordinate the complex interactions along the “brain-gut” axis to regulate multiple physiological functions (Morton et al., 2014). For example, vagally mediated feedback is critical to the neural control of food intake (Ahima et al., 1996; Hahn et al., 1998). Moreover, gastric distention triggers activities of the vagal afferent in a dose-dependent manner (Berthoud et al., 2001;

Powley and Phillips, 2004), suggesting the existence of mechanoreceptors in the GI tract to control meal size by monitoring volume or food load. In *Drosophila*, feeding is also under strict control, albeit with simpler anatomy (Edgecomb et al., 1994; Pool and Scott, 2014; Wang and Wang, 2019). The GI tract of the fly is also innervated with abundant descending neurons from the brain, including those releasing neuropeptides (Dus et al., 2015; Kuraishi et al., 2015). Most of the endocrine and neuropeptide systems that are known to control feeding in *Drosophila* are conserved in mammals (Jourjine, 2017).

The digestive tract in the adult fly receives innervation from two major sources: (1) the stomatogastric nervous system (SNS), including the corpus cardiacum and the hypercelebral ganglion, and (2) central neurons located at the pars intercerebralis (PI) of the brain and in the abdominal ganglion of the ventral nerve cord (Nässel et al., 2015). In the GI tract, most of the regions with muscle valves are innervated, consistent with the notion that regulating peristaltic GI movement is one of the main functions of intestinal neurons (Browning and Travagli, 2014). There is also experimental support for the notion that these neurons control feeding and digestion by coordinating GI tract movement. For instance, HGN1 neurons in the adult ventral nerve cord (VNC) innervate the hindgut to regulate defecation (Cognigni et al., 2011). A counterpart of those neurons in larvae (RN2 neurons) also regulates defecation (Zhang et al., 2014).

Although the cell bodies of most fly enteric neurons are not located on the GI tract, they are not necessarily efferent neurons that regulate GI tract movement (Cognigni et al., 2011). Sensory afferent neurons, especially those carrying mechanical cues, are of importance for the regulation of GI tract movement. Studies in several other insects have demonstrated the existence of stretch receptor neurons along the GI tract that monitor the volume of ingested food (Thomson and Holling, 1974; Yano et al., 1986). It remains an intriguing open question whether there are stretch receptor neurons in *Drosophila* and, if so, how these neurons sense stretch. Among the mechanotransduction channels, the Piezo family plays multiple roles in sensory transduction and development (Geng et al., 2017; Murthy et al., 2017; Wu et al., 2017; Xiao, 2020; Zhang et al., 2020). Mouse Piezo1 is involved in mechanical feedback that is critical for multiple physiological functions, including sensing shear stress of blood flow and regulating red blood cell volume (Cahalan et al., 2015; Zeng et al., 2018). In contrast, Piezo2 is found mainly in the nervous system of mice. Besides its predominant functions in mediating somatosensory touch (Ranade et al., 2014), it also senses airway stretch and coordinates lung inflation (Nonomura et al., 2017). However, it is unknown whether Piezo proteins participate in the acute regulation of food intake in the vagus nerve on the GI tract.

Here, we report that *Drosophila* crop distention induced by food intake delivers a fast and direct satiety signal to the brain to suppress further feeding. This feedback is mediated by a group of Piezo^{+} brain neuroendocrine neurons that innervate the crop wall. These neurons use Piezo as a sensor and are mechanosensitive. Moreover, they are also capable of releasing insulin-like peptides and other hormones. Our finding reveals how mechanical stimuli mediate fast feeding regulation, which may be coordinated with humoral control.

RESULTS

Mechanotransduction Channel Piezo Is Involved in Acute Feeding Control

To measure the meal size of an individual fly, we fed the flies with sugar solution until they became unresponsive to further sugar stimulation on the proboscis (MAFE assay) (Pool et al., 2014; Qi et al., 2015; Figure 1A). The total volume of consumption was then measured. Wild-type flies fasted for 4 h normally consumed 0.133 ± 0.033 μL of 100 mM sucrose solution, resulted in a moderately distended crop (Figures 1B and 1C; Video S1). The meal size was comparable at the two sugar concentrations tested (Figures 1B and S1A), suggesting the existence of a mechanical satiety signal from the crop that is distinct from taste and nutritional cues.

To investigate the molecular basis for this mechanical signal of satiety, we measured the meal size of mutants for the mechanosensitive ion channel Piezo. Strikingly, the *piezo* mutant ($piezo^{KO}$) flies consumed much more (0.374 ± 0.035 μL) than the control group (Figures 1B and 1C), leading to a noticeably bloated crop (Figure S1D) and abdomen (Figure 1C; Video S2). In the most severe cases, the mutant flies consumed so much that they exploded, reminiscent of the scene in the Monty Python film *The Meaning of Life* in which a person's stomach explodes because of gross overeating. Freely moving $piezo^{KO}$ flies also consumed significantly more food compared with wild-type flies (Figure S1C). The over-feeding behavior of $piezo^{KO}$ is independent of the sweet taste of sugar, as they also drank more water than control flies after being desiccated for 4 h (Figure S1A; Videos S3 and S4). Nor did the nutritional value of the food affect the phenotype, as the mutant flies consumed noticeably more sweet but calorie-free sugars such as L-glucose (Figure 1D), or nutritious but tasteless chemicals such as sorbitol (Figure 1E), compared with control flies. Furthermore, the amount of food intake is positively correlated with fasting time for both *piezo* mutant flies and wild-type flies (Figure S1E).

To avoid the influence on feeding by manual handling, we used an automatic feeding monitoring system (FlyPAD) (Itskov et al., 2014) to quantify the total sip duration of the flies within 20 min. $piezo^{KO}$ flies took more sips than wild-type control flies (Figures 1F and 1G). To establish a link between distention state (size of the crop) and rate of consumption, we monitored the flies' water drinking sips using FlyPAD. Sip frequency dropped after the first couple of minutes (Figure S1F), indicating a negative correlation between crop size and consumption rate.

We also performed experiments in which flies were fasted for 16 h on a piece of Kimwipe soaked with water. $piezo^{KO}$ flies consumed significantly more than wild-type flies in the MAFE assay (Figure S1G) or in the FlyPAD assay (Figure S1H). This result suggests that the overconsumption does not result from thirst. Additionally, the rhythm of midgut contraction was not significantly altered in $piezo^{KO}$ flies (Figures S1J–S1L), suggesting that the overconsumption phenotype of the mutant is not due to an acceleration of gut movement.

To validate that the feeding control defect is indeed due to the loss of Piezo function, we used piezo-Gal4 (Kim et al., 2012)to knock down *piezo* expression with a *piezo* RNAi line, leading to an over-feeding phenotype similar to that of $piezo^{KO}$ flies (Figure 1H;

Figure S1D). Conversely, overconsumption in *piezo*^{KO} flies can be rescued by expressing either *Drosophila* Piezo protein or mammalian Piezo1 protein (Figure 1I), suggesting an evolutionarily conserved function of Piezo proteins. Furthermore, we found that the channel conductivity of the Piezo protein is required for feeding control, as a non-conducting mutation of mPeizo1 (1–2,336) (Coste et al., 2015; Song et al., 2019) failed to rescue the overconsumption phenotype as full-length mouse Piezo1 or human Piezo1 did (Figure 1I). Taken together, our results demonstrate that Piezo mediates satiety signals to inhibit food intake independent of the taste or nutritional value of the food, supporting the notion that these signals arise from mechanical distension along the digestive tract during feeding.

Piezo^{+} Neurons Innervate the Crop of the Digestive Tract

To investigate how the mechanosensitive channel Piezo might regulate feeding, we examined the expression pattern of the Piezo protein using the piezo-Gal4 line. We observed arborizations of the Piezo+ neurons on the crop, an organ for initial food storage during feeding (Figures 2A and 2B). The neurites appeared to descend from the brain, branch on the proventriculus, and then extend to the crop along the crop duct. The nerve terminals arborize extensively to cover the crop wall (Figure 2C). Moreover, these neurites were stained positive for GFP in a piezo^{GFP} knockin fly (Figure S2A), indicating that they are sensory afferents that relay the information of the crop volume to the brain. The morphology and location of these Piezo^{+} neurons make them well positioned to sense volume change of the crop during feeding.

To uncover the identity of these neurons, we performed a screen to identify subsets of Piezo^{+} neurons that innervate the crop by intersecting the piezo-Gal4 with different LexA driver lines with FLP-recombinase-mediated recombination (Bohm et al., 2010). We found a Dilp2-LexA line that labels insulin-producing cells of the flies, when intersecting with piezo-Gal4, marked the crop Piezo^{+} neurons (Figure 2D). This Dilp2-LexA had an expression pattern similar to that of Dilp2-Gal4, which predominantly labels the insulin-producing cells (IPC neurons) in the PI region (Sakai et al., 2014), and this was further validated with double labeling of the Dilp2-LexA and Dilp2-Gal4 lines (Figure S2B). The neurons labeled with the Dilp2-LexA driver or the intersection between the Dilp2 and piezo drivers were stained positive for DILP2 (Figures S2C and S2E). These results indicate that the cell body clusters are Dilp2^{+} cells, and the Dilp2-LexA driver faithfully labels Dilp2^{+} cells. Furthermore, the neurites of the Dilp2-Gal4 were similar to those from the Piezo^{+} IPC neurons (Figures 2G–2I), indicating that the Piezo+ IPC neurons are a subset of Dilp2 neurons that innervate the crop.

The Piezo^{+} IPC neurons have their cell bodies located in the cluster of neuro-secretory cells at the PI region and send their neurites along the brain mid-line to reach the esophagus (Figures 2G and 2H). These neurites branch in the saddle of the subesophageal zone (SEZ) and then continue to traverse along the esophagus and the crop duct all the way to the crop wall (Figures 2F and 2I). To better characterize the neurites on the crop wall, we used Dilp2-Gal4 to drive the expression of Denmark and syt-GFP to label the dendrites and axons, respectively. The neurites on the crop wall express both dendritic and axonal markers (Figure 2J), indicating that the neurites are a mix of efferent and afferent nerves.

Piezo$^+$ IPC Neurons Are Required for Fast Feeding Control

We next asked whether the Piezo channel functions in Piezo$^+$ IPC neurons to prevent over-feeding by using Dilp2-Gal4 to specifically knock down Piezo expression in the IPC neurons. Reducing Piezo function only in IPC neurons resulted in overconsumption (Figure 3A) as severe as that of *piezo* mutant flies, supporting the notion that Piezo$^+$ IPC neurons are critical for mechanical feeding control.

Previous studies have demonstrated that insulin and IPC neurons play multifaceted roles in feeding regulation in *Drosophila* (Oh et al., 2019). However, acute effects of this regulation have not received much attention. As flies usually finish a meal in less than a minute (Yapici et al., 2016), we reasoned that crop distention that results from food influx activates Piezo$^+$ IPC neurons to terminate further food intake. To test this hypothesis, we introduced a temperature-sensitive dominant-negative form of dynamin (*shibire^{ts}*, *shi^{ts}*) to reversibly block synaptic transmission in IPC neurons. At the permissive temperature, the Dilp2-Gal4 > UAS-*shi^{ts}* flies consumed the normal amount of food (Figure 3B). In contrast, when tested under the restrictive temperature, they consumed markedly more food compared with the control group (Figure 3B). In a converse experiment, we used the warmth-sensitive cation channel TrpA1 (Hamada et al., 2008) to transiently activate IPC neurons at 30°C. The flies consumed significantly less compared with those at 22°C or control flies at either 22°C or 30°C (Figure 3C). Importantly, by intersecting Dilp2-LexA and Piezo-Gal4, we were able to manipulate the activity of only Piezo$^+$ IPC neurons. Acute block or activation of those neurons was sufficient to increase or decrease feeding, respectively (Figures 3D and 3E). Taken together, our results demonstrate that IPC neurons are both necessary and sufficient to convey rapid satiety signal during feeding to prevent overconsumption.

To achieve better temporal resolution of feeding behavior, we performed optogenetic experiments to test whether rapid activation or inhibition of IPCs affected feeding. When Dilp2 neurons expressing CsChrimson were activated with light, flies fed significantly less under the same fasting condition (Figure 3F). Additionally, light of stronger intensity produced more profound inhibition on feeding, indicating that the activity of IPC neurons is negatively correlated with feeding (Figure 3F). In contrast, when these neurons were inhibited by light-gated anion channel GtACR, the flies showed an overconsumption phenotype (Figure 3G).

There are 14–20 IPC neurons in the fly brain (Nässel et al., 2013; Ohhara et al., 2018; Figure S3). Among these, about 6 or 7 neurons are Dilp2$^+$/Piezo$^+$ (Figure 2H) and ~14 neurons are Dilp2$^+$/piezo$^-$ (Figure S2D). By using Piezo-LexA > LexAop-Gal80 to express CsChrimson only in the Dilp2$^+$/piezo$^-$ neurons, the inhibition of feeding was eliminated (Figure 3F). This result suggests that the Dilp2$^+$/piezo$^-$ neurons are not required for the mechanical inhibition of feeding.

To reveal the fine structures of individual Piezo$^+$/Dilp2$^+$ neurons that innervate the crop, we used heat-shock controlled flip-pase to stochastically label subsets of Dilp2$^+$ neurons (hs-Flp; UAS (FRT.stop) CsChrimson-mVenus/+; Dilp2-GAL4/+). Of 300 flies examined, there were seven brains with single-neuron labeling and neurites on the crop (Figure S2F). The neurites of the single neurons were much sparser compared with the projections

from Dilp2-GAL4 > UAS-GFP (Figures S2F and S2G). Importantly, compared with the intense coverage of the tritocerebrum of the SEZ in the Dilp2-Gal4 label neurons (Figure S2G), the single Piezo^{+}/Dilp2^{+} neurons each arborized a small area of the tritocerebrum. The projections were either uni-lateral (left panels) or bi-lateral (right panels). This result suggests that Piezo^{+}/Dilp2^{+} neurons may be integrated into the feeding circuits by synapsing onto the neurons that innervate the tritocerebrum of the SEZ.

DILP2 Is Dispensable for Fasting Feeding Control

To ask whether the secretion of DILPs plays a role in the regulation, we activated IPC neurons in the flies with *Dilp* mutants. Dilp2, 3, and 5, three principal hormones produced in IPC neurons (Post et al., 2018), appeared dispensable for acute feeding control, as neuronal activation in the mutant background also suppressed feeding (Figures S3A–S3C). Moreover, blood sugar level and body fat were not dramatically elevated because of overconsumption in the *piezo*^{KO} flies, indicating that metabolic regulation may be able to compensate for the excessive food intake (Figure S3D). To test whether fast mechanical distention of the crop triggers DILP2 release from IPC neurons, we quantified DILP2 protein by antibody immunostaining. The DILP2 level in IPC cell bodies was not significantly changed right after water consumption, indicating that mechanical distention was not sufficient to trigger DILP2 release, at least at the time point tested (Figure S3E). This is in agreement with the observation that knocking out Dilp2 did not cause an overconsumption phenotype.

Piezo^{+} IPC Neurons Respond to Crop Distention

Thus far, we have shown that a subset of the neuro-secretory IPC neurons mediates fast feeding termination, presumably by assessing crop fullness. To test whether Piezo^{+} IPC neurons can indeed sense mechanical distention, we monitored activity of the IPC neurons with an intracellular Ca2^{+} indicator, GCaMP6m (Chen et al., 2013). Initially we attempted to feed the flies with sugar solution while imaging the cell bodies of IPC neurons through a small window in the head capsule. However, flies under this imaging condition were not able to consume the amount of food that would cause satiety in normal flies, likely because of the injury from surgery. We thus devised an alternative approach: we inserted a pipette into the crop and inflated it with artificial *Drosophila* hemolymph (AHL) (Figure 4A). This method allows the rapid manipulation of crop volume (Figure 4A). Furthermore, this setup has the advantage of ruling out potential influence from peripheral sensory inputs that could occur in a feeding assay. By inflating the crop to a volume of about 0.25 μL, we observed an activation of the cell bodies of IPC neurons (Figure 4B; Video S5). This inflation-elicited Ca2^{+} elevation was largely diminished in the *piezo*^{KO} flies and was resumed by expressing Piezo with Dilp2-Gal4 in the mutant background (Figures 4C and 4D). These results demonstrate that IPC neurons are mechanosensitive and that the mechanosensitivity is dependent of the Piezo channel.

It was reported that the recurrent nerves (RNs) ascending from the digestive tract relay post-ingestive feedback to inhibit feeding (Dethier and Gelperin, 1967), as severing these nerve results in overconsumption in blowflies. We found that these nerves are labeled with Dilp2-Gal4. To ask whether these ascending nerves from the crop are indeed mechanosensitive, we performed Ca2^{+} imaging on these nerves at the cervical connective of the fly. These

nerves showed substantial increases in $Ca2^+$ level upon crop distention, and this activation depends on Piezo, as the response was not present in the *piezo*^{KO} flies (Figures 4E and 4F). Additionally, we tested whether feeding states regulate the mechanical response of Piezo$^+$ IPCs. The $Ca2^+$ responses were compared between fasted and fed flies (Figure 4D), indicating that humoral and mechanical regulations are separate.

DISCUSSION

Mechanical Regulation of Feeding

In this study, we have identified a group of neurons, Piezo$^+$ IPC neurons, that innervate the crop and use Piezo as a mechanosensor for monitoring the crop fullness. This mechanical information provides an important satiety signal to suppress feeding, which is essential to the animals, as it allows rapid control to avoid over-feeding (Figure 4G). Previously, several studies have found that food texture has a profound influence on the choice of food source, and food hardness is detected using multiple sensory structures on the labellum of the fly (Jeong et al., 2016; Sánchez-Alcañiz et al., 2017; Zhang et al., 2016). Moreover, mechanosensory neurons innervating the posterior compartments of the GI tract regulate feeding and defecation (Olds and Xu, 2014; Zhang et al., 2014). Our study provides further evidence for the importance of mechanosensation in food intake and disposal along the entire GI tract.

We observed two interesting features regarding the activation of Piezo$^+$ IPC neurons in response to crop distension. First, the extent of activation is not linearly proportional to crop volume. Instead, it becomes evident only when the crop is distended beyond a certain volume threshold, about 0.2 μL (Figure 4B). This feature is in accordance with our behavioral observation that flies continue to feed until the crop reaches a certain size, although the volume achieved with manual inflation is slightly larger than the volume a fly would consume in the feeding assay. Second, the activation shows slow adaption to prolonged crop distention, a feature distinct from the inactivation kinetics of Piezo channels and most of the known mechanoreceptors (Ranade et al., 2015), suggesting that a mechanism other than Piezo kinetics may exist to maintain the activity of Piezo+ IPC neurons to sustained crop distension.

Is mechanical regulation of feeding a conserved mechanism? Recent studies have demonstrated that intestinal mechanoreceptors play a key role in the regulation of feeding (Bai et al., 2019; Kim et al., 2020). Thus, a similar mechanism of feeding regulation seems to exist in both flies and mice. Whether the Piezo protein acts as the key mechanotransducer in the vagal mechanosensory neurons in vertebrates is an interesting open question.

Downstream Circuits of the GI Mechano-sensors

What might be the circuitry that relays the “fullness” signal from the Piezo$^+$ IPC mechanosensitive neurons to inhibit feeding? These neurons may target a circuit that directly terminates feeding. It is also possible that feeding inhibition is achieved by peptide release from these neurons. For the first scenario, candidates from previous work include but are not limited to the neural circuits in the SEZ that control volume of consumption (Joseph

et al., 2017; Pool et al., 2014; Yapici et al., 2016), SEZ neurons that balance food and water intake (Jourjine et al., 2016), and motor neurons in the SEZ that control proboscis extension and food pumping (Manzo et al., 2012; Schwarz et al., 2017). By comparing the arborizations of $Piezo^{+}/Dilp2^{+}$ neurons at SEZ with those of the four GABA neurons (DSOG1 neurons) identified by Scott's lab (Pool et al., 2014), we observed that they appeared to overlap in the ventral SEZ. This result supports the notion that "RN and DSOG1 neurons inhibit feeding by independent convergence onto feeding circuits" (Pool et al., 2014). For the second possibility, however, it would be more challenging to pinpoint the downstream circuits. IPC neurons release multiple peptides upon activation, and most of these peptides work in a dispersing manner to modulate neurons not in synaptic contact with these peptidergic neurons (Nässel et al., 2013; Semaniuk et al., 2018). As the feeding regulation by $Piezo^{+}$ IPC neurons we have observed is relatively fast (usually within 1 min) and is independent of Dilp2, 3, or 5, it seems more plausible that $Piezo^{+}$ IPC neurons may affect the downstream circuitry through direct synaptic input. IPC neurons have been found to arborize in the dorsal tritocerebrum region of the SEZ immediately below the esophagus. As the ventral part of the SEZ, the tritocerebrum is innervated by neurons from the mouthparts, the pharynx, and the stomatogastric system (Rajashekhar and Singh, 1994). Whereas the central roles of the tritocerebrum to integrate gustatory information in feeding control have been well documented (Rajashekhar and Singh, 1994), whether and how mechanical cues from IPC neurons and other circuits are incorporated into this brain region require future investigation.

Coordination between Mechanical and Humoral Regulation of Feeding

We have shown that mechanical satiety signal plays an indispensable role in acute feeding control of flies. Notably, the hunger and satiety states of flies are controlled by diverse molecules and neural circuits. For example, Dilp2 functions as a satiety signal to control feeding by modulating multiple neural circuits (Liu et al., 2015; Semaniuk et al., 2018; Zhao and Campos, 2012). Another neuropeptide MIP was also found to mediate satiety signals to terminate feeding (Min et al., 2016). Furthermore, amino acid-specific satiety seems to be differentially regulated from that of sugar-induced satiety (Yang et al., 2018). Taken together, satiety is represented by a combination of humoral signals as well as distention of the GI tract. The mechanical satiety pathway uncovered in our study seems to be independent of the taste or nutritional value of the food, indicating that it might work in parallel with the humoral pathways, possibly with different timescales. Interestingly, mechanical stimulation alone from food-induced gastric distention is insufficient to terminate ingestion in humans. Rather, it contributes to satiety when acting in concert with pregastric and postgastric stimuli (Cummings and Overduin, 2007). Hence, although the mechanical regulation of satiety is a shared mechanism in different species, the complexity of the regulation may differ.

STAR★METHODS

RESOURCE AVAILABILITY

Lead Contact—Further information and requests for resources and reagents should be directed to and will be fulfilled by the Lead Contact, Wei Zhang (wei_zhang@mail.tsinghua.edu.cn)

Materials Availability—All unique/stable reagents (fly lines, plasmids) generated in this study are available from the Lead Contact without restriction.

Data and Code Availability—The code generated during this study are available at GITHUB: https://github.com/EBGU/Cap2Sip

EXPERIMENTAL MODEL AND SUBJECT DETAILS

Animals—Fruit fly *Drosophila melanogaster* strains were maintained with a 12 h/12 h light/dark cycle at 25°C (unless otherwise noted) and 60% humidity (PERCIVAL incubator). w^{1118} strain (BDSC:5905) was used as wild-type control. Fly stocks were raised in non-crowded conditions on standard cornmeal medium. Fly food consisted of (per 1 L) 10 g agar, 7.25 g sucrose, 30 g glucose, 24.5 g yeast, 50 g corn meal, 17.5ml methyl 4-hydroxybenzoate, 4ml propionic acid. Female flies of 4–7 days old were used in the experiments.

The following fly lines were used: $piezo^{KO}$ ((Bloomington stock center) BL58770), *UAS-Piezo-RNAi* (Vienna *Drosophila* RNAi Center, 105132), *UAS-DmPiezo* (BL58773), *Piezo-Gal4* (BL59266), $UAS(FRT.stop)shibire^{ts}$ (BL66675 and BL66676), *UAS-dTRPA1*(BL26263 and BL26264), *UAS-GCaMP6m* (BL42748), $UAS\text{-}Shibire^{ts}$ (gift from Yi Zhong at Tsinghua University, China), *UAS-hPiezo1*, *UAS-mPiezo1* (gift from Ardem Patapoutian at Scripps, USA), *UAS-mPiezo1–1-2336, Piezo-GFP*^{KI} (gift from Yuanquan Song at University of Pennsylvania, USA), *Dilp2-GAL4*, *LexAOP-Flp, UAS(FRT.stop)dTRPA1, UAS(FRT.stop)CsChrimson-mVenus* (gift from Yufeng Pan at Southeast University, China), *ilp3, ilp5 mutant strains* (gift from Yan Zhu at the Institute of Biophysics, China), *Dilp2-LexA, ilp2 mutant strain* (gift from Yan Li at the Institute of Biophysics, China).

METHOD DETAILS

Generation of transgenic flies—Piezo-LexA was generated by the HACK method (Lin and Potter, 2016). The pHACK-G4 > LexA plasmid was modified from pHACK-G4 > QF2 vector (Addgene plasmid#: 80275) by replacing the QF2 element with the LexA element. Then the donor plasmid was injected into embryos (w-; +/+; piezo-Gal4/nos-Cas9). Insertions were confirmed with both PCR and RFP signals in the compound eyes.

Temporal and Volumetric Consumption Assays—Flies were collected upon eclosion and aged for 4–7 days. For food deprivation, female flies were kept in an empty vial for 4 hr without food and water. Fasted flies were then mounted onto glass slides with nail polish and allowed to recover in a humidified chamber for 2 hr. Individual flies were presented

with a glass micropipette (ASONE micro pipette, 1 μL) filled with test solutions (MAFE assay (Qi et al., 2015)). Flies were fed until they showed no more PER for the test solutions in five consecutive touch of forelegs or if they started to regurgitate. The residual length was then measured to calculate the consumed volume: $\left(\frac{totallength - residuallength}{totallength}\right)$ μL. Food dye (ShiTou, Brilliant Blue) was added to the solutions in the some of the experiments to visualize the crop distention.

For free feeding assay, fasted flies (starved for 6 hr) were fed with dye-stained food for 30 min. Consumption was calculated by measuring the average body weight change of 50 flies in each genotype.

Feeding assay with FlyPAD (Fly Proboscis and Activity Detector)—FlyPAD assay was carried out as previously described (Itskov et al., 2014) with slight modifications. Flies were collected upon eclosion and aged for 4–7 days. For food deprivation, female flies were kept in an empty vial with filter paper soaked with water for 16 hr. Each fly was transferred to one feeding chamber on the FlyPAD board. Feeding was recorded for 20 min. Sips were detected with Python codes (Cap2Sip) translated from the MATLAB codes (Itskov et al., 2014). Cumulative sips duration was calculated as the summation of all sips detected along the 20 min time window.

Crop size measurement—Female flies were starved for 16 hr and fed on 100 mM sucrose with food dye for 30 min. The crop was dissected out in PBS and mounted between two pieces of cover glass with two spacers of 0.18 mm. The crop was slightly pressed to form a “pie” shape with the same thickness of the spacer. Images were taken under a Nikon SMZ71 stereo-microscope with a Basler LAN camera. The area was measured with ImageJ and the volume was calculated as $V = area * thickness$.

Midgut peristalsis assay—Peristalsis of the midgut was monitored with the Bellymount method (Koyama et al., 2020). Brief, female flies were fed with 100 mM with food dye until the dye was visible along the whole intestine. Flies were mounted between two coverslips with their lateral abdomen facing upward so that the midgut was visible. Videos were taken at 30 fps. Videos were converted to image series with ImageJ. An ROI was taken at the midgut area and the gut movement frequency was calculated from the change of intensity of food dye in that ROI.

Optogenetics and thermogenetics—Newly eclosed flies were collected and transferred into food containing a piece of filter paper with 500 μL of sugar-retinal solution (500 μM all-trans-retinal diluted in 100 mM sucrose solution) on the surface (Inagaki et al., 2014). Flies were kept in darkness and used for optogenetics experiments after fed with all-trans-retinal 3 to 5 days. Light intensity was measured with Laser power meter LP1 (Sanwa, Japan).

For heat activation experiments, flies were kept in an incubator of 22°C. Prior to experiments, flies were transferred onto a metal bath that was pre-heated to 30°C.

Immunohistochemistry—Immunostaining was conducted according to previous protocol (Hu et al., 2019). The following antibodies were used: rabbit anti-GFP (1: 1000, Invitrogen), rabbit anti-mcherry (1:1000, Rockland) and mouse anti-nc82 (1:500, Developmental Studies Hybridoma Bank). Secondary antibodies were Alexa Fluor 555 goat anti-rabbit IgG (1: 500, Invitrogen), Alexa Fluor 488 goat anti-rabbit IgG (1: 500, Invitrogen), Alexa Fluor 647 goat anti-mouse IgG (1: 500, Invitrogen), Rabbit anti-DILP2 (gift from Yan Li at the Institute of Biophysics, China) and Alexa 555-Phalloidin (1:200, Solarbio). Images were acquired with a Zeiss LSM 780, Olympus FV1000 or Andor Dragonfly with 2 μm optical sections at a resolution of 1024 × 1024 pixels or 2048 × 2048 pixels.

To test whether fast mechanical distention of the crop triggers DILP2 release from the IPC, the DILP2 protein was quantified by antibody immunostaining against DILP2. The flies were desiccation for 4h. Each fly was manually fed with water until it stopped drinking. The fly was frozen on ice immediately after it stopped drinking. Control flies were frozen on ice without water feeding. The brains were then dissected out in PBS for DILP2 staining (1:1000). The samples were processed in parallel and using the same solution and imaged with the same laser power and scanning settings.

Stochastic labeling of Dilp2 neurons—Virgin hs-Flp females were crossed with Dilp2-Gal4; UAS(FRT.stop)CsChrimson-mVenus males at 25°C. Heat shock was performed in a 37°C water bath for 10 min when early pupae began to form. Brains and crops of four to six days old flies dissected out and stained using rabbit anti-GFP and nc82 as mentioned above.

Calcium Imaging—Adult flies 5–7 days old were starved for 4–6 hr to empty their crop prior to the experiment. The flies were fed with a small amount of water to enlarge their crop for easier visualization. For imaging of fed flies, the starved flies were allowed to feed on a piece of filter paper soaked with 100 mM sucrose until their abdomen were bloated. All legs and wings were removed to exclude the interference on calcium recording due to movement. The fly was then fixed on a Sylgard-coated dish with three fine tungsten pins on the head, thorax and lower abdomen. The preparation was immersed in the artificial hemolymph-like solution (AHL) (Ruta et al., 2010). The PI region of the brain was exposed by cutting a small window in the posterior head cuticle. The preparation was then transferred to the imaging microscope. The pipette (150–120-69, Sutter Instrument CO.) was pulled on a P-97 puller to a diameter of 20μm and was connected to a manual injector by rubber tube to inflate or deflate the crop. GCaMP signals from the cell bodies of IPCs were detected by an Olympus FV1000 confocal microscope with a 40x water objective. Images were acquired at 1 frame per second at a resolution of 512 × 512 pixels. The volume changes of the crop were monitored with a 4X lens before and after the stimulation. The volume was calculated from the sphere diameter of the distended crop.

For recurrent nerve (RN) imaging, a fly was fixed on a Sylgard-coated dish with two fine tungsten pins on the head and the lower abdomen. GCaMP signals from the RN at the cervical connective were detected by a Zyla Flash 4.2 CMOS camera on an Olympus BX51Wi microscope with a 32X air objective. Images were processed with ImageJ.

Body Triglyceride and Sugar Measurement

For metabolic measurement, both satiated flies and fasted flies (starve for 6h) were measured. Female flies were collected upon eclosion and aged for 5 days. Six female flies were homogenized in 500 μL in PBS with 0.2% Triton-X and incubated at 70°C for 5 min to inactivate endogenous enzymes. The homogenates were then centrifuged at 12000 rpm for 15 min at 4°C and 150 μL supernatant was collected for subsequent measurement. For triglyceride (TAG) assays, the following kits were used: Sigma TG reagent (T2449), Free Glycerol Reagent (F6428), Glycerol standard (G7793). 10 μL supernatant was added to either 20 μL TG reagent or 20 μL PBS and incubated at 37°C for 20 min. 100 μL Free Glycerol reagent was added to each of them and incubated at 37°C for 5 min before OD value was measured at 540 nm. TAG amounts were determined from the total glycerol present in the sample treated with the Triglyceride reagent. TAG levels were normalized to protein amounts in each homogenate using a Bradford assay (Sigma Bradford Reagent, B6916). For sugar assays, the following kits were used: Megazyme Trehalose (E-TREH) and D-Glucose Assay kit (K-GLUC). 10 μL supernatant was added to either 20 μL PBS solution or 19.8 μL PBS solution with 0.2 μL trehalase, incubate at 37°C for 20 min. 150 μL D-Glucose Assay kit was added to each of them and incubated at 37°C for 5 min before OD value was measured at 510 nm. Trehalose and glucose levels were also normalized to protein amounts.

QUANTIFICATION AND STATISTICAL ANALYSIS

Statistical analysis was performed with Prism (GraphPad Software). All datasets were presented as mean ± SEM. Significance was determined by comparison to the indicated control group using unpaired Student’s t test or between groups using One-way ANOVA. Following ANOVA analysis, the Tukey post hoc test was conducted to determine statistical significance.

Supplementary Material

Refer to Web version on PubMed Central for supplementary material.

ACKNOWLEDGMENTS

We thank members of the Zhang lab for discussions. We thank Dr. Bailong Xiao for technical support and discussions. We thank Yanli Zhang and the Imaging Core Facility, Technology Center for Protein Sciences of Tsinghua University for assistance using Dragonfly. This work was supported by grant 31871059 from the National Natural Science Foundation of China, grant Z181100001518001 from the Beijing Municipal Science and Technology Commission, a “Brain+X” Seeds grant from the IDG/McGovern Institute for Brain Research at Tsinghua to W.Z., and NIH grant 1R35NS97227 to Y.N.-J. W.Z. is an awardee of the Young Thousand Talent Program of China. Y.N.-J. is an investigator of the Howard Hughes Medical Institute.

REFERENCES

Ahima RS, Prabakaran D, Mantzoros C, Qu D, Lowell B, Maratos-Flier E, and Flier JS (1996). Role of leptin in the neuroendocrine response to fasting. Nature 382, 250–252. [PubMed: 8717038]

Asher G, and Sassone-Corsi P (2015). Time for food: the intimate interplay between nutrition, metabolism, and the circadian clock. Cell 161, 84–92. [PubMed: 25815987]

Bai L, Mesgarzadeh S, Ramesh KS, Huey EL, Liu Y, Gray LA, Aitken TJ, Chen Y, Beutler LR, Ahn JS, et al. (2019). Genetic identification of vagal sensory neurons that control feeding. Cell 179, 1129–1143.e23. [PubMed: 31730854]

Berthoud H-R, Lynn PA, and Blackshaw LA (2001). Vagal and spinal mechanosensors in the rat stomach and colon have multiple receptive fields. Am. J. Physiol. Regul. Integr. Comp. Physiol. 280, R1371–R1381. [PubMed: 11294756]

Bohm RA, Welch WP, Goodnight LK, Cox LW, Henry LG, Gunter TC, Bao H, and Zhang B (2010). A genetic mosaic approach for neural circuit mapping in *Drosophila*. Proc. Natl. Acad. Sci. U S A 107, 16378–16383. [PubMed: 20810922]

Browning KN, and Travagli RA (2014). Central nervous system control of gastrointestinal motility and secretion and modulation of gastrointestinal functions. Compr. Physiol. 4, 1339–1368. [PubMed: 25428846]

Cahalan SM, Lukacs V, Ranade SS, Chien S, Bandell M, and Patapoutian A (2015). Piezo1 links mechanical forces to red blood cell volume. eLife 4, e07370.

Chen T-W, Wardill TJ, Sun Y, Pulver SR, Renninger SL, Baohan A, Schreiter ER, Kerr RA, Orger MB, Jayaraman V, et al. (2013). Ultrasensitive fluorescent proteins for imaging neuronal activity. Nature 499, 295–300. [PubMed: 23868258]

Cognigni P, Bailey AP, and Miguel-Aliaga I (2011). Enteric neurons and systemic signals couple nutritional and reproductive status with intestinal homeostasis. Cell Metab. 13, 92–104. [PubMed: 21195352]

Coste B, Murthy SE, Mathur J, Schmidt M, Mechioukhi Y, Delmas P, and Patapoutian A (2015). Piezo1 ion channel pore properties are dictated by C-terminal region. Nat. Commun. 6, 7223. [PubMed: 26008989]

Cummings DE, and Overduin J (2007). Gastrointestinal regulation of food intake. J. Clin. Invest. 117, 13–23. [PubMed: 17200702]

Dethier VG, and Gelperin A (1967). Hyperphagia in the blowfly. J. Exp. Biol. 47, 191–200.

Dus M, Lai JS, Gunapala KM, Min S, Tayler TD, Hergarden AC, Geraud E, Joseph CM, and Suh GS (2015). Nutrient sensor in the brain directs the action of the brain-gut axis in *Drosophila*. Neuron 87, 139–151. [PubMed: 26074004]

Edgecomb RS, Harth CE, and Schneiderman AM (1994). Regulation of feeding behavior in adult *Drosophila* melanogaster varies with feeding regime and nutritional state. J. Exp. Biol. 197, 215–235. [PubMed: 7852903]

Gao Y, Shuai Y, Zhang X, Peng Y, Wang L, He J, Zhong Y, and Li Q (2019). Genetic dissection of active forgetting in labile and consolidated memories in *Drosophila*. Proc. Natl. Acad. Sci. U S A 116, 21191–21197. [PubMed: 31488722]

Geng J, Zhao Q, Zhang T, and Xiao B (2017). In touch with the mechanosensitive Piezo channels: structure, ion permeation, and mechanotransduction. Curr. Top. Membr. 79, 159–195. [PubMed: 28728816]

Hahn TM, Breininger JF, Baskin DG, and Schwartz MW (1998). Coexpression of Agrp and NPY in fasting-activated hypothalamic neurons. Nat. Neurosci. 1, 271–272. [PubMed: 10195157]

Hamada FN, Rosenzweig M, Kang K, Pulver SR, Ghezzi A, Jegla TJ, and Garrity PA (2008). An internal thermal sensor controlling temperature preference in *Drosophila*. Nature 454, 217–220. [PubMed: 18548007]

Hu Y, Wang Z, Liu T, and Zhang W (2019). Piezo-like gene regulates locomotion in *Drosophila* larvae. Cell Rep. 26, 1369–1377.e4. [PubMed: 30726723]

Inagaki HK, Jung Y, Hoopfer ED, Wong AM, Mishra N, Lin JY, Tsien RY, and Anderson DJ (2014). Optogenetic control of *Drosophila* using a red-shifted channelrhodopsin reveals experience-dependent influences on courtship. Nat Methods 11, 325–332. [PubMed: 24363022]

Itskov PM, Moreira JM, Vinnik E, Lopes G, Safarik S, Dickinson MH, and Ribeiro C (2014). Automated monitoring and quantitative analysis of feeding behaviour in *Drosophila*. Nat. Commun. 5, 4560. [PubMed: 25087594]

Jeong YT, Oh SM, Shim J, Seo JT, Kwon JY, and Moon SJ (2016). Mechanosensory neurons control sweet sensing in *Drosophila*. Nat. Commun. 7, 12872. [PubMed: 27641708]

Joseph RM, Sun JS, Tam E, and Carlson JR (2017). A receptor and neuron that activate a circuit limiting sucrose consumption. eLife 6, e24992. [PubMed: 28332980]

Jourjine N (2017). Hunger and thirst interact to regulate ingestive behavior in flies and mammals. BioEssays 39, 1600261.

Jourjine N, Mullaney BC, Mann K, and Scott K (2016). Coupled sensing of hunger and thirst signals balances sugar and water consumption. Cell 166, 855–866. [PubMed: 27477513]

Kim SE, Coste B, Chadha A, Cook B, and Patapoutian A (2012). The role of *Drosophila* Piezo in mechanical nociception. Nature 483, 209–212. [PubMed: 22343891]

Kim KS, Seeley RJ, and Sandoval DA (2018). Signalling from the periphery to the brain that regulates energy homeostasis. Nat. Rev. Neurosci. 19, 185–196. [PubMed: 29467468]

Kim DY, Heo G, Kim M, Kim H, Jin JA, Kim HK, Jung S, An M, Ahn BH, Park JH, et al. (2020). A neural circuit mechanism for mechanosensory feedback control of ingestion. Nature 580, 376–380. [PubMed: 32296182]

Koyama LAJ, Aranda-Díaz A, Su YH, Balachandra S, Martin JL, Ludington WB, Huang KC, and O'Brien LE (2020). Bellymount enables longitudinal, intravital imaging of abdominal organs and the gut microbiota in adult *Drosophila*. PLoS Biol. 18, e3000567. [PubMed: 31986129]

Kuraishi T, Kenmoku H, and Kurata S (2015). From mouth to anus: functional and structural relevance of enteric neurons in the *Drosophila* melanogaster gut. Insect Biochem. Mol. Biol. 67, 21–26. [PubMed: 26232723]

Li Q, and Gong Z (2015). Cold-sensing regulates *Drosophila* growth through insulin-producing cells. Nat. Commun. 6, 10083. [PubMed: 26648410]

Lin CC, and Potter CJ (2016). Editing transgenic DNA components by inducible gene replacement in *Drosophila* melanogaster. Genetics 203, 1613–1628. [PubMed: 27334272]

Liu Y, Luo J, Carlsson MA, and Nässel DR (2015). Serotonin and insulin-like peptides modulate leucokinin-producing neurons that affect feeding and water homeostasis in *Drosophila*. J. Comp. Neurol. 523, 1840–1863. [PubMed: 25732325]

Manzo A, Silies M, Gohl DM, and Scott K (2012). Motor neurons controlling fluid ingestion in *Drosophila*. Proc. Natl. Acad. Sci. U S A 109, 6307–6312. [PubMed: 22474379]

Min S, Chae HS, Jang YH, Choi S, Lee S, Jeong YT, Jones WD, Moon SJ, Kim YJ, and Chung J (2016). Identification of a peptidergic pathway critical to satiety responses in *Drosophila*. Curr. Biol. 26, 814–820. [PubMed: 26948873]

Mohammad F, Stewart JC, Ott S, Chlebikova K, Chua JY, Koh TW, Ho J, and Claridge-Chang A (2017). Optogenetic inhibition of behavior with anion channelrhodopsins. Nat. Methods 14, 271–274. [PubMed: 28114289]

Morton GJ, Meek TH, and Schwartz MW (2014). Neurobiology of food intake in health and disease. Nat. Rev. Neurosci. 15, 367–378. [PubMed: 24840801]

Murthy SE, Dubin AE, and Patapoutian A (2017). Piezos thrive under pressure: mechanically activated ion channels in health and disease. Nat. Rev. Mol. Cell Biol. 18, 771–783. [PubMed: 28974772]

Nässel DR, Kubrak OI, Liu Y, Luo J, and Lushchak OV (2013). Factors that regulate insulin producing cells and their output in *Drosophila*. Front. Physiol. 4, 252. [PubMed: 24062693]

Nässel DR, Liu Y, and Luo J (2015). Insulin/IGF signaling and its regulation in *Drosophila*. Gen. Comp. Endocrinol. 221, 255–266. [PubMed: 25616197]

Nonomura K, Woo SH, Chang RB, Gillich A, Qiu Z, Francisco AG, Ranade SS, Liberles SD, and Patapoutian A (2017). Piezo2 senses airway stretch and mediates lung inflation-induced apnoea. Nature 541, 176–181. [PubMed: 28002412]

Oh Y, Lai JS-Y, Mills HJ, Erdjument-Bromage H, Giammarinaro B, Saadipour K, Wang JG, Abu F, Neubert TA, and Suh GSB (2019). A glucose-sensing neuron pair regulates insulin and glucagon in *Drosophila*. Nature 574, 559–564. [PubMed: 31645735]

Ohhara Y, Kobayashi S, Yamakawa-Kobayashi K, and Yamanaka N (2018). Adult-specific insulin-producing neurons in *Drosophila* melanogaster. J. Comp. Neurol. 526, 1351–1367. [PubMed: 29424424]

Olds WH, and Xu T (2014). Regulation of food intake by mechanosensory ion channels in enteric neurons. eLife 3, e04402.

Pool AH, and Scott K (2014). Feeding regulation in *Drosophila*. Curr. Opin. Neurobiol. 29, 57–63. [PubMed: 24937262]

Pool AH, Kvello P, Mann K, Cheung SK, Gordon MD, Wang L, and Scott K (2014). Four GABAergic interneurons impose feeding restraint in *Drosophila*. Neuron 83, 164–177. [PubMed: 24991960]

Post S, Karashchuk G, Wade JD, Sajid W, De Meyts P, and Tatar M (2018). *Drosophila* insulin-like peptides DILP2 and DILP5 differentially stimulate cell signaling and glycogen phosphorylase to regulate longevity. Front. Endocrinol. (Lausanne) 9, 245.

Powley TL, and Phillips RJ (2004). Gastric satiation is volumetric, intestinal satiation is nutritive. Physiol. Behav. 82, 69–74. [PubMed: 15234593]

Qi W, Yang Z, Lin Z, Park JY, Suh GS, and Wang L (2015). A quantitative feeding assay in adult *Drosophila* reveals rapid modulation of food ingestion by its nutritional value. Mol. Brain 8, 87. [PubMed: 26692189]

Rajashekhar KP, and Singh RN (1994). Neuroarchitecture of the tritocerebrum of *Drosophila* melanogaster. J. Comp. Neurol. 349, 633–645. [PubMed: 7860793]

Ranade SS, Woo S-H, Dubin AE, Moshourab RA, Wetzel C, Petrus M, Mathur J, Bé gay V, Coste B, Mainquist J, et al. (2014). Piezo2 is the major transducer of mechanical forces for touch sensation in mice. Nature 516, 121–125. [PubMed: 25471886]

Ranade SS, Syeda R, and Patapoutian A (2015). Mechanically activated ion channels. Neuron 87, 1162–1179. [PubMed: 26402601]

Ruta V, Datta SR, Vasconcelos ML, Freeland J, Looger LL, and Axel R (2010). A dimorphic pheromone circuit in *Drosophila* from sensory input to descending output. Nature 468, 686–690. [PubMed: 21124455]

Sakai T, Watanabe K, Ohashi H, Sato S, Inami S, Shimada N, and Kitamoto T (2014). Insulin-producing cells regulate the sexual receptivity through the painless TRP channel in *Drosophila* virgin females. PLoS ONE 9, e88175. [PubMed: 24505416]

Sánchez-Alcañiz JA, Zappia G, Marion-Poll F, and Benton R (2017). A mechanosensory receptor required for food texture detection in *Drosophila*. Nat. Commun 8, 14192. [PubMed: 28128210]

Schwarz O, Bohra AA, Liu X, Reichert H, VijayRaghavan K, and Pielage J (2017). Motor control of *Drosophila* feeding behavior. eLife 6, e19892. [PubMed: 28211791]

Semaniuk UV, Gospodaryov DV, Feden'ko KM, Yurkevych IS, Vaiserman AM, Storey KB, Simpson SJ, and Lushchak O (2018). Insulin-like peptides regulate feeding preference and metabolism in *Drosophila*. Front. Physiol. 9, 1083. [PubMed: 30197596]

Song Y, Li D, Farrelly O, Miles L, Li F, Kim SE, Lo TY, Wang F, Li T, Thompson-Peer KL, et al. (2019). The mechanosensitive ion channel Piezo inhibits axon regeneration. Neuron 102, 373–389.e6. [PubMed: 30819546]

Sun J, Liu C, Bai X, Li X, Li J, Zhang Z, Zhang Y, Guo J, and Li Y (2017). *Drosophila* FIT is a protein-specific satiety hormone essential for feeding control. Nat. Commun. 8, 14161. [PubMed: 28102207]

Thomson AJ, and Holling CS (1974). Experimental component analysis of blowfly feeding behaviour. J. Insect Physiol. 20, 1553–1563. [PubMed: 4851973]

Travers JB, Travers SP, and Norgren R (1987). Gustatory neural processing in the hindbrain. Annu. Rev. Neurosci. 10, 595–632. [PubMed: 3551765]

Wang GH, and Wang LM (2019). Recent advances in the neural regulation of feeding behavior in adult *Drosophila*. J. Zhejiang Univ. Sci. B 20, 541–549.

Williams EK, Chang RB, Strochlic DE, Umans BD, Lowell BB, and Liberles SD (2016). Sensory neurons that detect stretch and nutrients in the digestive system. Cell 166, 209–221. [PubMed: 27238020]

Wu J, Lewis AH, and Grandl J (2017). Touch, tension, and transduction-the function and regulation of Piezo ion channels. Trends Biochem. Sci. 42, 57–71. [PubMed: 27743844]

Wu S, Guo C, Zhao H, Sun M, Chen J, Han C, Peng Q, Qiao H, Peng P, Liu Y, et al. (2019). Drosulfakinin signaling in fruitless circuitry antagonizes P1 neurons to regulate sexual arousal in *Drosophila*. Nat. Commun. 10, 4770. [PubMed: 31628317]

Xiao B (2020). Levering mechanically activated Piezo channels for potential pharmacological intervention. Annu. Rev. Pharmacol. Toxicol. 60, 195–218. [PubMed: 31454291]

Xu B, and Xie X (2016). Neurotrophic factor control of satiety and body weight. Nat. Rev. Neurosci. 17, 282–292. [PubMed: 27052383]

Yang Z, Huang R, Fu X, Wang G, Qi W, Mao D, Shi Z, Shen WL, and Wang L (2018). A post-ingestive amino acid sensor promotes food consumption in *Drosophila*. Cell Res. 28, 1013–1025. [PubMed: 30209352]

Yano T, Nakashima M, Takashima A, and Shiraishi A (1986). The roles of the recurrent nerve and the ventral nerve cord in the feeding response of the blowfly, Phormia regina M. Exp. Biol. 46, 37–44. [PubMed: 3817111]

Yapici N, Cohn R, Schusterreiter C, Ruta V, and Vosshall LB (2016). A taste circuit that regulates ingestion by integrating food and hunger signals. Cell 165, 715–729. [PubMed: 27040496]

Zeng WZ, Marshall KL, Min S, Daou I, Chapleau MW, Abboud FM, Liberles SD, and Patapoutian A (2018). PIEZOs mediate neuronal sensing of blood pressure and the baroreceptor reflex. Science 362, 464–467. [PubMed: 30361375]

Zhang W, Yan Z, Li B, Jan LY, and Jan YN (2014). Identification of motor neurons and a mechanosensitive sensory neuron in the defecation circuitry of *Drosophila* larvae. eLife 3, e03293.

Zhang YV, Aikin TJ, Li Z, and Montell C (2016). The basis of food texture sensation in *Drosophila*. Neuron 91, 863–877. [PubMed: 27478019]

Zhang L, Yu J, Guo X, Wei J, Liu T, and Zhang W (2020). Parallel mechanosensory pathways direct oviposition decision-making in *Drosophila*. Curr. Biol. 30, 3075–3088.e4. [PubMed: 32649914]

Zhao XL, and Campos AR (2012). Insulin signalling in mushroom body neurons regulates feeding behaviour in *Drosophila* larvae. J. Exp. Biol. 215, 2696–2702. [PubMed: 22786647]

Zhou C, Pan Y, Robinett CC, Meissner GW, and Baker BS (2014). Central brain neurons expressing doublesex regulate female receptivity in *Drosophila*. Neuron 83, 149–163. [PubMed: 24991959]

Highlights

- Mechano-gated ion channel Piezo is required for fast feeding control in flies
- A group of Piezo-expressing neurons monitor crop volume during feeding
- Piezo-expressing neurons are activated directly by crop distension

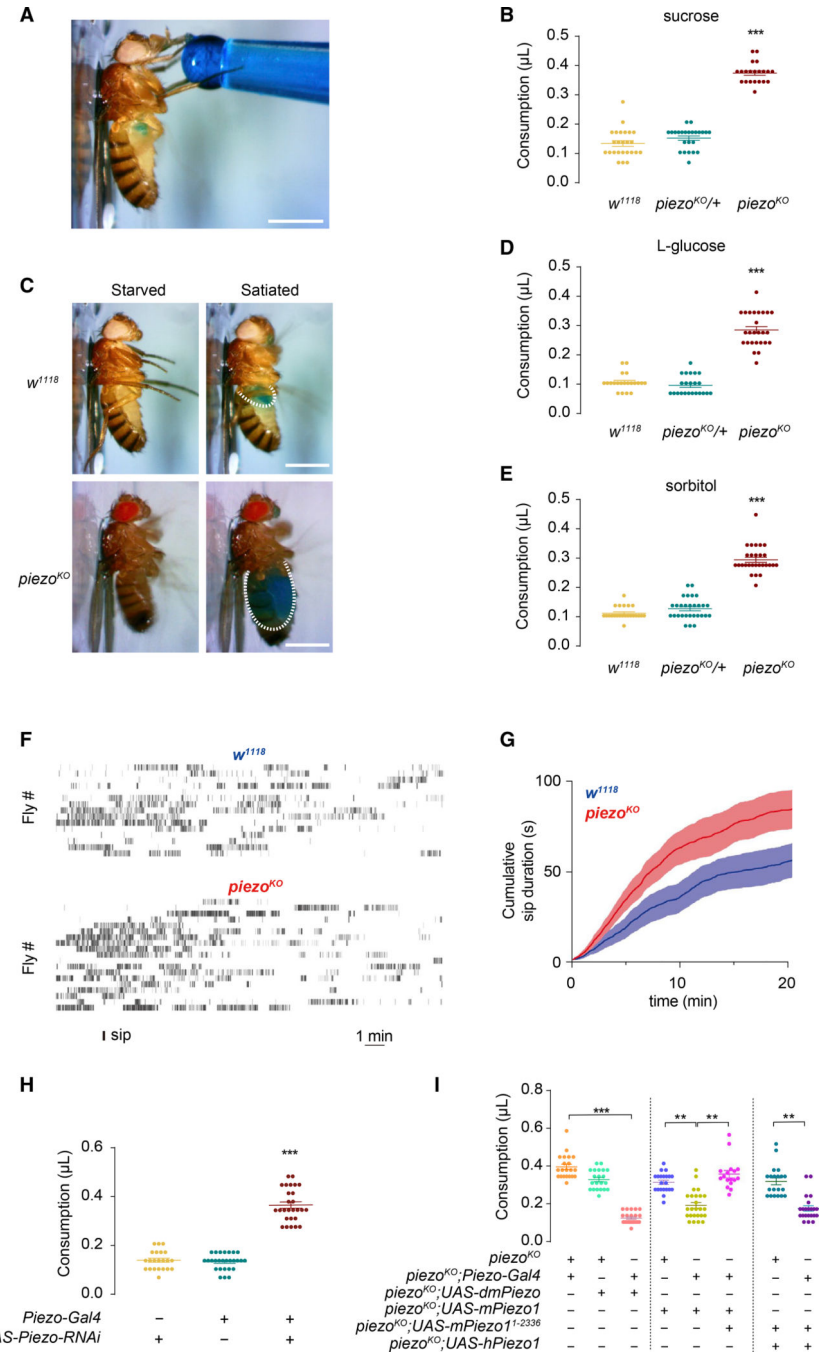

Figure 1. Mechanosensitive Channel Piezo Is Required in Acute Feeding Control

(A) Consumption volume of sugar solution of individual fly. Blue dye was added to visualize crop distention. Scale bar, 1 mm.

(B) Wild-type (WT) flies and *piezo*^{KO} flies starved for 4 h were fed with 100 mM sucrose. n = 20–30; each point represents data from a single fly; mean ± SEM; ***p < 0.001, one-way ANOVA, Tukey post hoc.

(C) WT flies and *piezo*^{KO} flies starved for 4 h were fed with blue-dyed sugar solution. Two different states are shown: starved (pre-feeding) and satiated (post-feeding) state. Dashed line outlines crop size after feeding. Scale bar, 1 mm.

(D and E) WT flies and *piezo*^{KO} flies starved for 4 h were fed with 100 mM L-glucose and 100 mM sorbitol, respectively. n = 20–30; each point represents data from a single fly; mean ± SEM; ***p < 0.001, one-way ANOVA, Tukey post hoc.

(F and G) WT flies and *piezo*^{KO} flies starved for 4 h were assay on the FlyPAD. (F) Each vertical bar represents a single sip. (G) Cumulative sips durations were plotted over 20 min. n = 15 for WT and 19 for *piezo*^{KO}.

(H) Piezo knockdown by applying a *Piezo-Gal4*-driven *UAS-Piezo-RNAi* increased consumption. Tested with 100 mM sucrose solution. n = 20–30; mean ± SEM; ***p < 0.001, one-way ANOVA, Tukey post hoc.

(I) Over-feeding phenotype was rescued by expressing fly or mammalian Piezo1 proteins with Piezo-Gal4. n = 20–30; each point represents data from a single fly; mean ± SEM; ***p < 0.001, one-way ANOVA, Tukey post hoc.

See also Figure S1.

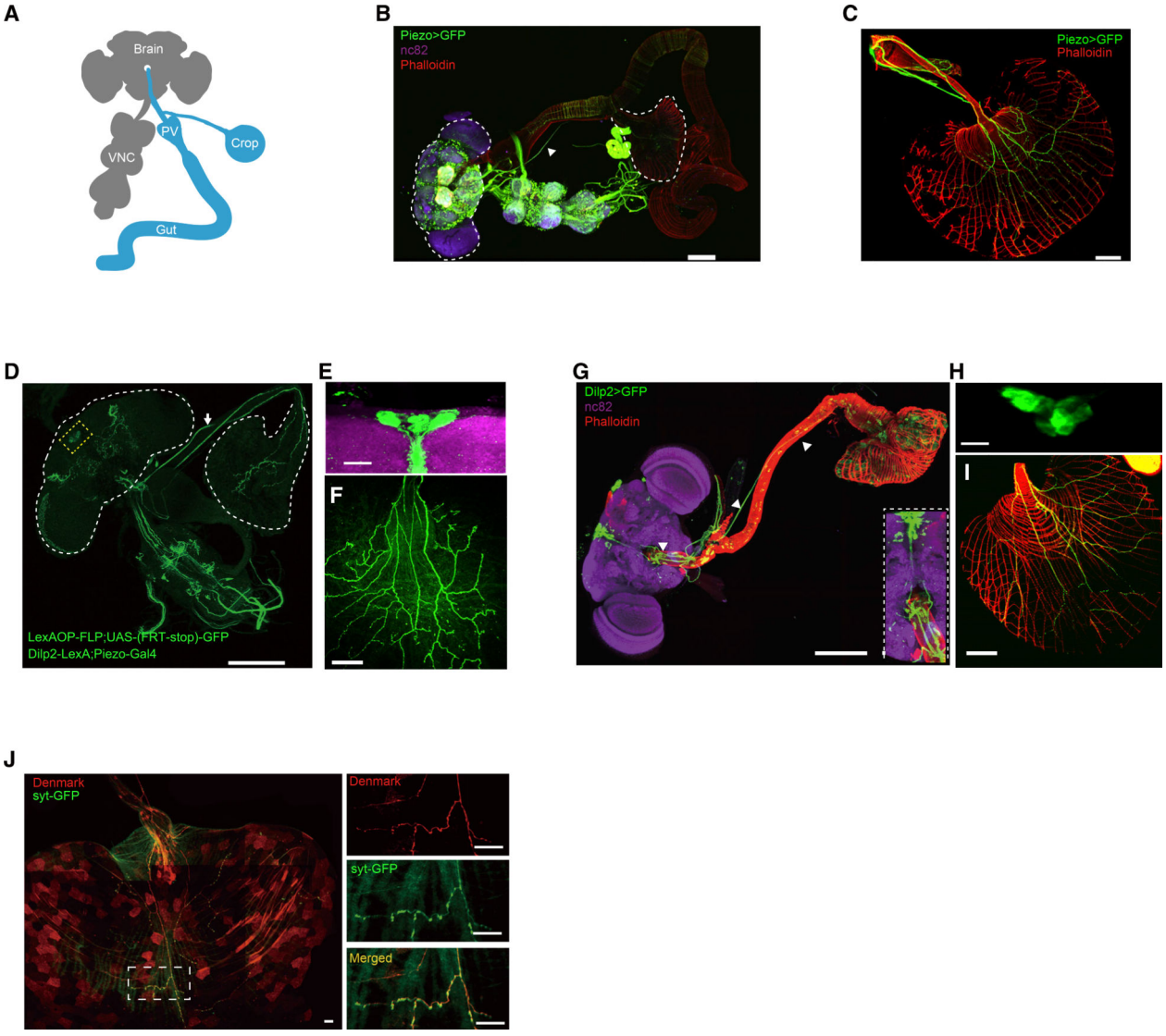

Figure 2. Piezo+ Neurons Innervate the Crop

(A) The central nervous system (brain and VNC, in gray color) and the anterior compartments of the digestive tract (foregut, midgut, and crop, in cyan color). PV, proventriculus.

(B) *Piezo-Gal4* drives expression of GFP in the brain, VNC, proventriculus, and crop. Scale bar, 200 μm. Brain and VNC were counter-stained with the neuropil marker nc82 (magenta). White arrow indicates Piezo+ crop projection neurons. Dashed lines outline the brain (left) and crop (right).

(C) Innervation of Piezo^{+} neurons on the crop wall. Smooth muscles are visualized with phalloidin (red). Scale bar, 200 μm.

(D–F) Intersection between *Dilp2-LexA* and *Piezo-Gal4*. (D) Yellow boxed region indicates Piezo+ IPCs. White arrow indicates crop projection neurons. Dashed lines outline the brain (left) and crop (right). Scale bar, 200 μm. (E) Cell bodies in the PI region. Scale bar, 20 μm. (F) Innervation on the crop wall. Scale bar, 200 μm..

(G–I) *Dilp2-Gal4* drives expression of GFP in the brain and crop. IPC neurons directly innervate the crop. Note the direct projection to IPC (arrows and inset). Brain and VNC were counter-stained with the neuropil marker nc82 (magenta). Smooth muscles are visualized with phalloidin (red). Scale bar, 200 μm. (H) Cell bodies in the PI region. Scale bar, 20 μm. (I) Innervation on the crop wall. Scale bar, 200 μm.

(J) *Dilp2-Gal4* drives expression of Denmark and syt-GFP in the neural arborizations on the crop. Scale bar, 50 μm.

See also Figure S2.

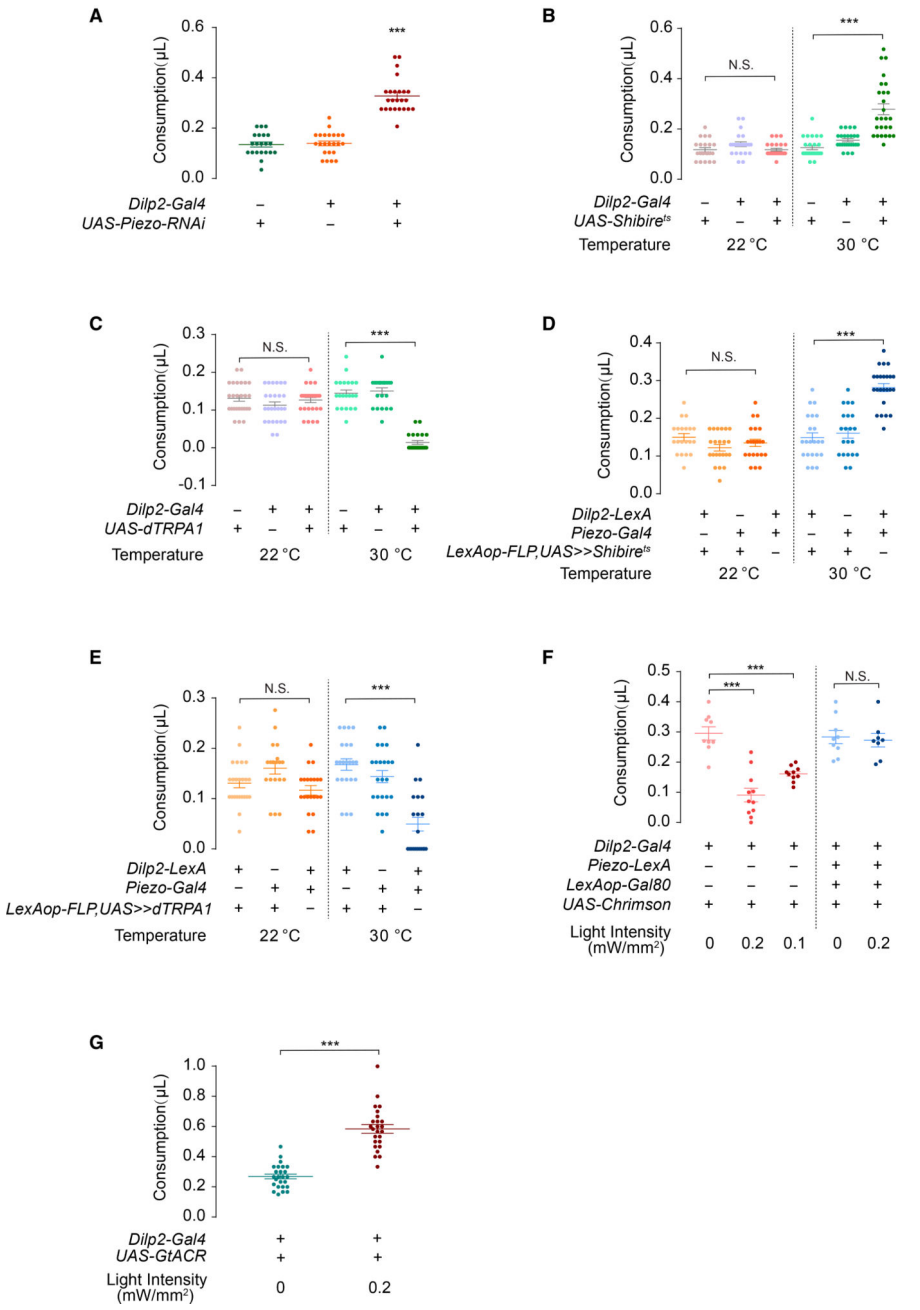

Figure 3. Piezo^{+} IPC Neurons Function in Feeding Regulation

(A) Piezo knockdown by *Dilp2-Gal4* increased food consumption. Tested with 100 mM sucrose solution. n = 20–30; box-and-whisker plot, whiskers mark minimum and maximum; each point represents data from a single fly; ***p < 0.001, one-way ANOVA, Tukey post hoc.

(B) IPC neurons inactivation with *shibire^{ts}* caused overconsumption at 30°C. Tested with 100 mM sucrose solution. n = 20–30; each point represents data from a single fly; mean ± SEM; ***p < 0.001, one-way ANOVA, Tukey post hoc.

(C) IPC neurons activation with *dTRPA1* caused decreased consumption. Tested with 100 mM sucrose solution. n = 20–30; each point represents data from a single fly; mean ± SEM***p < 0.001,; one-way ANOVA, Tukey post hoc.
(D and E) Intersectional inactivation or activation between *Dilp2-LexA* and *piezo-Gal4* with *shibire*^{ts} or *dTRPA1*. n = 20–30; mean ± SEM; ***p < 0.001, one-way ANOVA, Tukey post hoc.
(F) Piezo^{+} but not piezo^{-} IPC neuron activation with *CsChrimson* caused decreased consumption. Tested with 100 mM sucrose solution. n = 9–11; each point represents data from a single fly; mean ± SEM; ***p < 0.001, one-way ANOVA, Tukey post hoc.
(G) IPC neuron inhibition with *GtACR* caused overconsumption. Tested with 100 mM sucrose solution. n = 25; each point represents data from a single fly; mean ± SEM; ***p < 0.001, t test.
See also Figure S3.

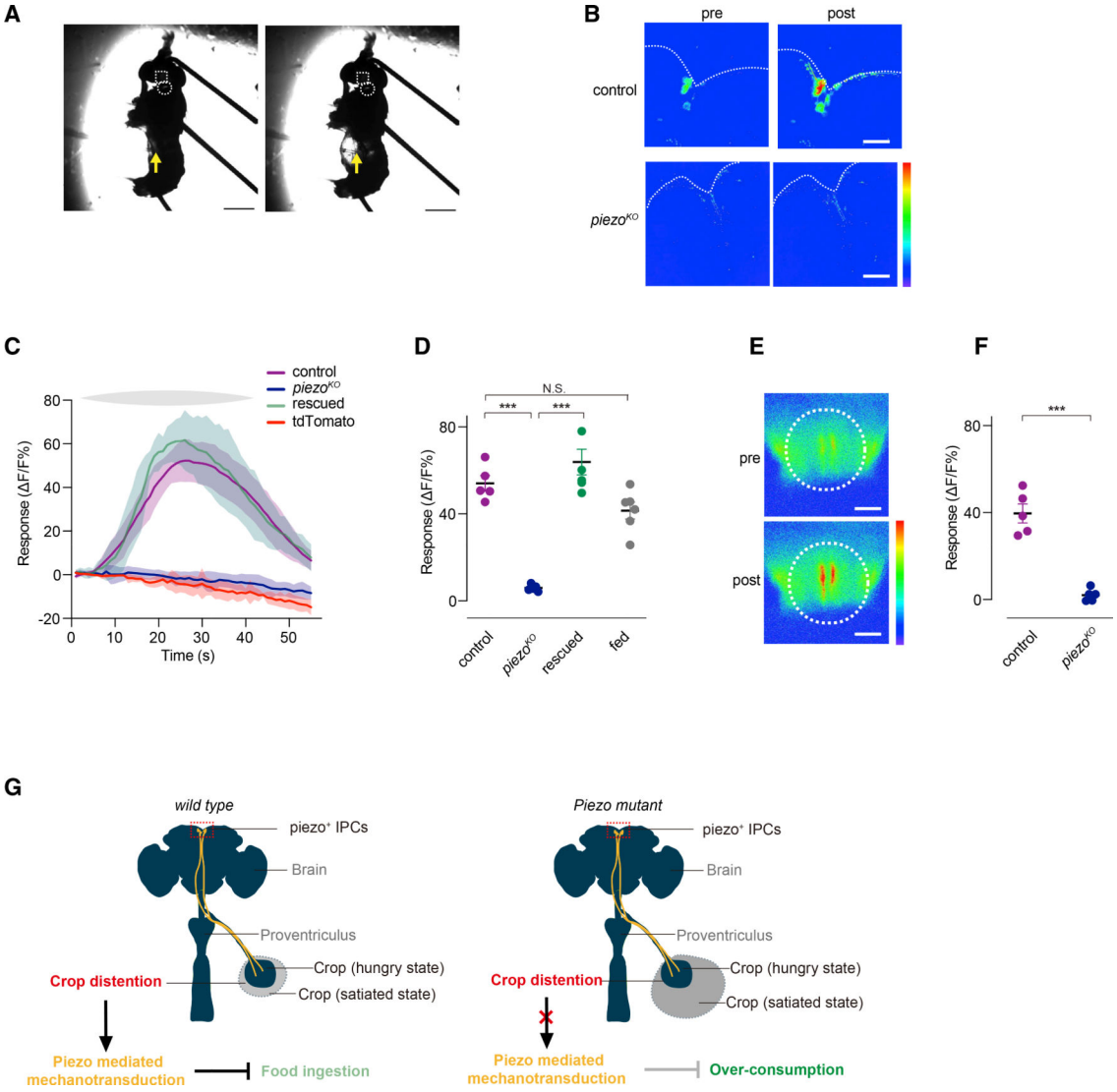

Figure 4. Piezo^{+} IPC Neurons Are Activated by Crop Distention

(A) Imaging setup with manual manipulation of crop volume. The upper panel shows a crop without distention, and in the lower panel the crop was inflated toa certain volume to mimic satiated post-feeding state. White boxes in both panels indicate the small window in the cuticle to expose PI brain region. White circles indicate the recurrent nerves (RNs) at the cervical connective. Yellow arrow indicates the pipette inserted into the crop. Scale bar, 500 μm.

(B) Representative GCaMP6m response of IPC neurons in control flies (upper panels) and *piezo^{KO}* mutant (lower panels). Crop distention activated IPC neurons (*UAS-GCaMP6m*, *UAS-tdTOM/Dilp2-Gal4*) but failed to do so in the *piezo^{KO}* mutant flies (*piezo^{KO}*; *UAS-GCaMP6m*, *UAS-tdTOM/Dilp2-Gal4*). Scale bar, 50 μm.

(C) Ca^{2+} response (ΔF/F) of IPC neurons in control, *piezo^{KO}* mutant, and rescued flies (*piezo^{KO}*; *UAS-GCaMP6m*, *UAS-tdTomato/Dilp2-Gal4*, *UAS-Piezo*). tdTomato was plotted as a control. Gray bar indicates crop distension.

(D) Peak response of IPC neurons to crop distension in IPC neurons in control, *piezo*^{KO} mutant, and rescued and fed control flies. n = 5–7, mean ± SEM, ***p < 0.001, t test. N.S., not significant.

(E and F) Peak response of RNs to crop distension in control and *piezo*^{KO} flies. n = 5–7, mean ± SEM, ***p < 0.001, t test. Scale bar, 100 μm.

(G) Working model for the function of Piezo in feeding control.

KEY RESOURCES TABLE

REAGENT or RESOURCE	SOURCE	IDENTIFIER
Antibodies		
Mouse monoclonal anti-nc82	Developmental Studies Hybridoma Bank	RRID: AB_2314866
Rabbit polyclonal anti-GFP	Invitrogen	A11122, RRID:AB_221569
Rabbit polyclonal anti-mCherry	Rockland	RRID:AB_2614470
Alexa 555-conjugated goat anti-rabbit IgG	Invitrogen	Cat # A21428, RRID:AB_2535849
Alexa 647-conjugated goat anti-mouse IgG	Invitrogen	Cat # A21235, RRID:AB_2535804
Alexa 488-conjugated goat anti-rabbit IgG	Invitrogen	Cat # A11008, RRID:AB_143165
Mouse anti-DILP2	Yan Li at the Institute of Biophysics, China (Sun etal., 2017)	N/A
TRITC Phalloidin	Solarbio	CA1610–300T
Chemicals, Peptides, and Recombinant Proteins		
Food dye (Brilliant blue)	ShiTou	N/A
Critical Commercial Assays		
Sigma TG reagent	Sigma	T2449
Free Glycerol Reagent	Sigma	F6428
Glycerol standard	Sigma	G7793
Sigma Bradford Reagent	Sigma	B6916
Trehalase	Megazyme	E-TREH
D-Glucose Assay kit	Megazyme	K-GLUC
Experimental Models: Organisms/Strains		
piezo ^{KO}	Bloomington *Drosophila* Stock Center	RRID:BDSC_58770
Piezo^{GFP} knock in	Yuanquan Song at U Penn (Song et al., 2019)	N/A
UAS-mPiezo1–1-2336	Yuanquan Song at U Penn (Song et al., 2019)	N/A
UAS-dmPiezo	Bloomington *Drosophila* Stock Center	RRID:BDSC_58773
Piezo-Gal4	Bloomington *Drosophila* Stock Center	RRID:BDSC_59266
Piezo-LexA	This paper	N/A
UAS(FRT.stop)shibire^{ts}	Bloomington *Drosophila* Stock Center	RRID:BDSC_66676
UAS(FRT.stop)shibire^{ts}	Bloomington *Drosophila* Stock Center	RRID:BDSC_66675
UAS-Piezo-RNAi	Vienna *Drosophila* RNAi Center	RRID:VDRC 105132
UAS-dTRPA1	Bloomington *Drosophila* Stock Center	RRID:BDSC_26263
UAS-CsChrimson	Bloomington *Drosophila* Stock Center	RRID:BDSC 55136
UAS-GtACR1	Adam Claridge-Chang (Mohammad et al., 2017)	N/A
UAS-dTRPA1	Bloomington *Drosophila* Stock Center	RRID:BDSC 26264
UAS-GCaMP6m	Bloomington *Drosophila* Stock Center	RRID:BDSC 42748
UAS-DenMark, UAS-syt.eGFP	Bloomington Drosophila Stock Center	RRID:BDSC 33064
UAS-mCherry.NLS	Bloomington *Drosophila* Stock Center	RRID:BDSC 38424
UAS-*shibire*^{ts}	Yi Zhong at Tsinghua University (Gao et al., 2019)	N/A
UAS-hPiezo1	Yuanquan Song at U Penn (Song et al., 2019)	N/A

REAGENT or RESOURCE	SOURCE	IDENTIFIER
UAS-mPiezo1	Yuanquan Song at U Penn (Song et al., 2019)	N/A
Dilp2-GAL4	Bloomington *Drosophila* Stock Center	RRID:BDSC 37516
LexAOP-Flp	Bloomington *Drosophila* Stock Center	RRID:BDSC 55819
UAS(FRT.stop)dTRPA1	Chuan Zhou at the Institute of Zoology, China (Zhou etal., 2014)	N/A
UAS(FRT.stop)CsChrimson-mVenus	Yufeng Pan at Southeast University, Chhina (Wu etal., 2019)	N/A
Dilp2 mutant strain	Bloomington *Drosophila* Stock Center	RRID:BDSC 30881
Dilp3 mutant strain	Bloomington *Drosophila* Stock Center	RRID:BDSC 30882
Dilp5 mutant strain	Bloomington *Drosophila* Stock Center	RRID:BDSC 30884
Dilp2-LexA	Yan Li at the Institute of Biophysics, China (Li and Gong, 2015)	N/A
Recombinant DNA		
pHACK-G4 > LexA	This paper	N/A
pHACK-G4 > QF2	Addgene	Plasmid#: 80275
Software and Algorithms		
Fiji	NIH Image	https://imagej.nih.gov/ij/
Graphpad Prism 6	GraphPad Software, La Jolla, CA	https://www.graphpad.com/scientific-software/prism/
Anaconda+	Anaconda Inc.	https://www.anaconda.com/
Cap2Sip	This paper	https://github.com/EBGU/Cap2Sip